Kamil Kazmierski*, Kamil Dominiak and Grzegorz Marut

Positioning performance with dual-frequency low-cost GNSS receivers

https://doi.org/10.1515/jag-2022-0042
Received September 28, 2022; accepted February 1, 2023;
published online February 22, 2023

Abstract: In this study, positioning quality is tested with the use of low-cost in-house developed receivers. The analyzes consider the practical use of low-cost devices in surveying works. In the network solution, the accuracy of the GNSS positioning based on low-cost receivers can be characterized by the repeatability of the baseline length of 1 and 6 mm in 24 h and 10 min observation sessions, respectively. The field experiment of 4 GNSS receivers and 3 GNSS low-cost receivers allowed for establishing a precise geodetic control network. The accuracy of the control point coordinates determined with low-cost GNSS receivers equals a maximum of 17 and 40 mm for the horizontal and height components, respectively. Therefore, low-cost GNSS receivers can provide positioning accuracy at the some centimeter level and can support land surveying and geodetic monitoring activities.

Keywords: geodetic control network; low-cost GNSS; multi-GNSS; u-blox.

1 Introduction

The basic applications of Global Navigation Satellite Systems (GNSS), such as positioning, navigation, and time transfer, have expanded extensively to new areas. These areas include monitoring continental plate movement [1], GNSS reflectometry [2], troposphere and ionosphere [3, 4] monitoring, landslides control [5, 6], or sea level measurements [7]. The increase in the application potential is related, among other things, to the increase in the number and decrease in the prices of GNSS receivers. In 2029, the number of GNSS receivers will exceed 2.6 billion, of which up to 90% will be devices whose cost will not exceed $150 [8]. Development and miniaturization open up new possibilities for GNSS chipsets widely available in everyday devices, starting with mobile phones and sports watches [8] and ending with clothes equipped with a small GNSS locator [9, 10]. Mobile phones gained even more potential in 2016 when Google reported the availability of raw GNSS data for Android 7 Nougat users [11]. This caused the smartphone potential and the area of application to be still growing [12]. The relative positioning accuracy of smartphones in short 20 min sessions can reach the horizontal decimeter accuracy and vertical component accuracies exceeding 2 m [13]. Precise Point Positioning [14] results based on mobile phones may even provide accuracies of 37 and 51 cm for horizontal and vertical components, respectively [15]. The use of the observation quality information of the observations provided by smartphones can also reduce the positioning quality [16].

Small chipsets designed only for tracking GNSS observations constitute another, more specialized group of low-cost receivers. Initially, low-cost receivers were able to track the single GNSS frequency L1 and, according to the ISO 17123-8 standard, ensured uncertainties of 5.5 and 11 mm for the horizontal and vertical components, respectively. These results are twice worse than the results for geodetic-grade instruments [17]. However, the Real-Time Kinematic (RTK) experiment for single-frequency low-cost receivers indicates centimeter-level accuracy in the kinematic mode [18]. Correct ambiguity fixing in RTK single frequency solution can reduce the horizontal error from approximately 2 m to about 0.05 m [19]. These accuracies and limited purchase costs allow for the establishment of more measurement points in surveying and geodetic networks [20] and the discovery of other application areas, such as ionosphere monitoring [21]. The single frequency was a limitation for PPP applications [22]; therefore, double differences for long vectors were preferred to obtain high accuracies [23]. The

***Corresponding author: Kamil Kazmierski**, Wrocław University of Environmental and Life Sciences, Institute of Geodesy and Geoinformatics, Grunwaldzka 53, 50-357 Wrocław, Poland,
E-mail: kamil.kazmierski@upwr.edu.pl. https://orcid.org/0000-0002-7927-9416
Kamil Dominiak and Grzegorz Marut, Wrocław University of Environmental and Life Sciences, Institute of Geodesy and Geoinformatics, Grunwaldzka 53, 50-357 Wrocław, Poland,
E-mail: kamil.dominiak5@gmail.com (K. Dominiak),
grzegorz.marut@upwr.edu.pl (G. Marut). https://orcid.org/0000-0001-9877-1898 (G. Marut)

newer two-frequency receivers showed a horizontal error of 3 mm and a vertical error of 8 mm in relative positioning [24]. The main limiting factor for low-cost GNSS sets is the patch antenna [25] which is often replaced during experiments by more sophisticated constructions [26]. The upgrade of GNSS antennas leads to millimeter positioning accuracy on a zero-baseline approach [27]. Additionally, a low-cost patch antenna requires dedicated corrections to the carrier phase pattern [28]. State-of-the-art dual-frequency low-cost receivers can track GPS, GLONASS, Galileo, and BeiDou signals.

As low-cost dual-frequency GNSS receivers have been available for a short time, the number of studies on the subject is small. No literature position discusses positioning results from a large group of low-cost GNSS receivers. Most existing research focuses on single baselines [29] or a couple of receivers treated as an RTK set [30, 31]. Furthermore, other studies often relate to navigation rather than classical surveying or geodetic measurements [32]. Therefore, this paper provides a comprehensive performance evaluation of a dual-frequency low-cost multi-GNSS receiver in relative and absolute positioning. Such an evaluation may increase the popularity of the use of low-cost GNSS receivers in everyday life of surveyors, e.g., in works connected to the establishment of geodetic control networks or setting up multiple low-cost receivers for monitoring vast land subsidence.

This study aims to investigate the measurement potential of low-cost GNSS receivers. The quality of the baselines determined in the differential GNSS static positioning is characterized and verified from the perspective of precise surveying requirements. The works are concluded by an experiment consisting of setting up a geodetic control network twice, with the use of geodetic-grade receivers and a set in which three devices were replaced with low-cost GNSS receivers.

2 Methodology

The experiment data were collected using the set of 11 low-cost u-blox C099-F9P receivers equipped with high precision GNSS ZED-F9P chipset and the default patch antenna ANN-MB supported by microcomputer and GSM modem. The Raspberry Pi is responsible for controlling the C099-F9P receiver and allows for remote configuration of the device through the Internet connection available via the Wi-Fi module or in the absence of a Wi-Fi network with the use of the GSM network. All those elements together with the power supply unit are enclosed in the hermetic box. The above-mentioned components are presented in Figure 1. Table 1 summarizes the signals stored in the Receiver Independent Exchange (RINEX) 3.04 format by the low cost receiver. The receiver and antenna are able to retrieve dual-band multi-GNSS frequencies for four GNSS constellations. The phase center offset (PCO) and phase center variation (PCV) accuracies declared by the manufacturer are also listed in Table 1. However, [28] derived a different set of PCO and PCV, which differs substantially from the values declared by the manufacturer. Due to these differences in calibrations data, it was decided to omit the calibration of antennas for low-cost receivers during computations.

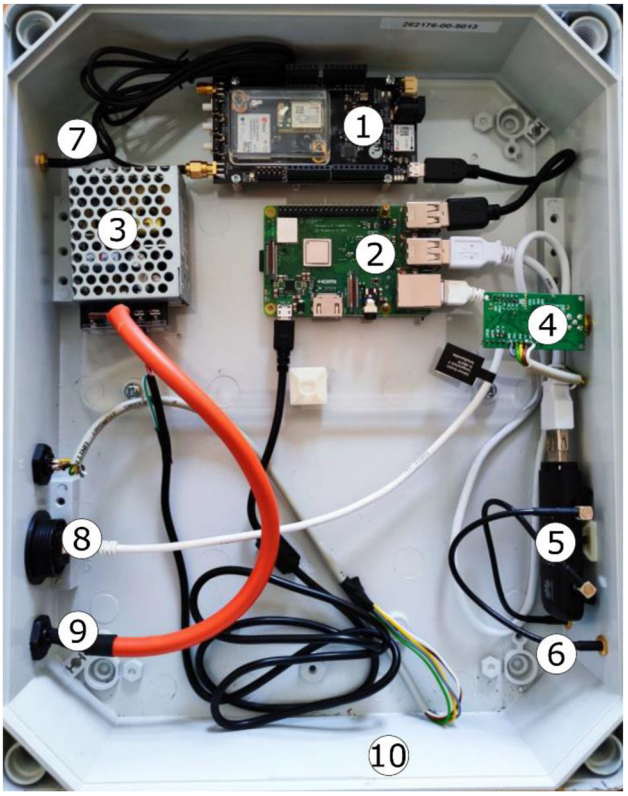

Figure 1: Low-cost dual-frequency GNSS receiver components.
1 – C099-F9P, 2 – Raspberry Pi, 3 – power supply unit, 4 – Wi-Fi module, 5 – GSM module, 6 – GSM antenna connector, 7 – GNSS antenna connector, 8 – 230 V Ethernet connector, 9 – AC 230 V input, 10 – hermetic enclosure.

In the experiment static data were collected at 15 locations. Most data were collected during one week between 22 and 28 March, 2021 (DoY 81–87) in the urban area of Wroclaw. Additionally, we used data recorded by 4 receivers between 14 and 20 September, 2020 (DoY 258–264) to provide data for long baseline computation. The receivers were distributed partly on the roofs of the buildings, and the tripods were installed at the ground level. To determine baselines created with low-cost and geodetic-grade receivers in the experiment Polish EUREF Permanent Network (EPN) stations were also used in the experiment. The last data set consists of geodetic grade receivers of the small regional network. Figure 2 shows the distribution of the u-blox receivers, geodetic grade receivers, and the Polish EUREF Permanent Network (EPN) stations used in the experiment. All receivers tracked the GPS, GLONASS and Galileo constellations with a 30 s interval with no additional mask for elevation angle or DOP. The prototype low-cost receivers used in tests could track up to 32 satellites simultaneously, and four-constellation tracking caused random gaps in satellite's observations. Due to these limitations, we decided to turn off BeiDou constellation tracking.

Table 1: GNSS signal supported by the u-blox ZED-F9P equipped with the ANN-MB series patch antenna.

Constellation	Tracked signals	PCO	PCV
GPS	L1 C/A (C/L1C), L2 C (C/L2C)	<5 mm horizontal <8.9 mm (L1) vertical <7.6 mm (L2) vertical	<5 mm (L1) <10 mm (L2)
GLONASS	L1 OF (C/L1C), L2 OF (C/L2C)	–	–
Galileo	E1-B/C (C/L1C), E5b (C/L7Q)	–	–
BeiDou	B1 (C/L1I), B2 (C/L7I)	–	–

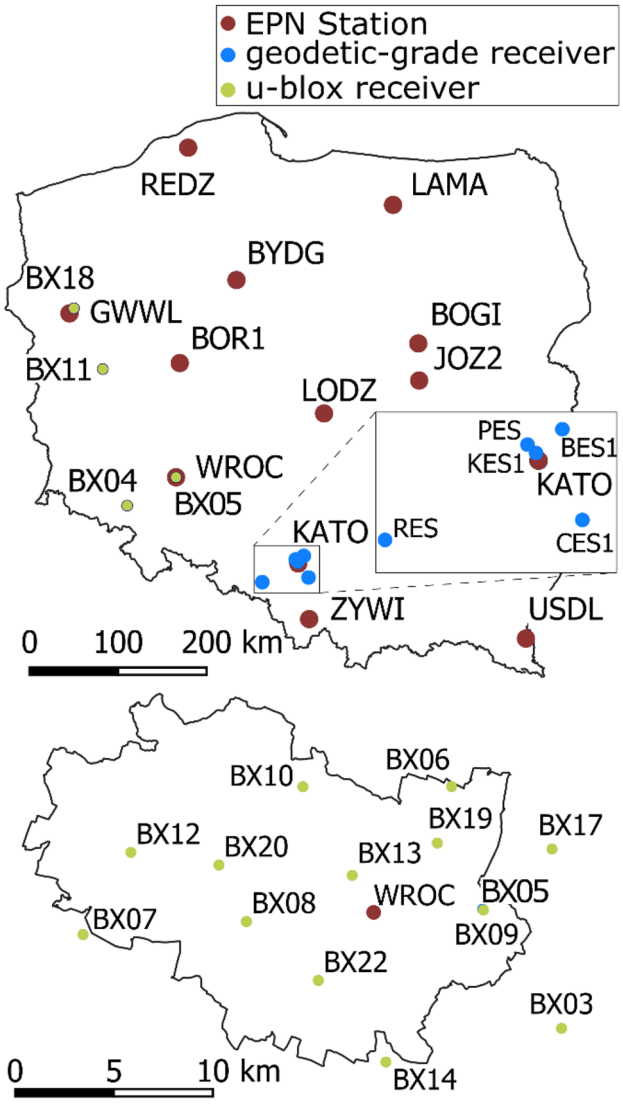

Figure 2: Distribution of low-cost receivers (gren dots), geodetic-grade receivers (blue dots), and EPN stations (red dots) during experiment campaigns. The upper plot shows the area of Poland, while the bottom plot covers the Wroclaw area.

3 Analysis of the collected observations

Figure 3 shows the percentage of epochs available during measurement campaigns with the use of low-cost receivers. As a reference value, 2880 observation epochs were adopted, which corresponds to data recording every 30 s during the day. The RINEX files saved by the low-cost receivers contain almost all the intervals, at the mean level close to 100%. The only exception is point BX12 with temporal data unavailability due to power supply problems which last about 2.5 h, resulting in availability of 90%. However, from the user's point of view, the completeness of the epochs saved in the RINEX files is not the only important factor. The user should also know what set of GNSS observations is available when performing calculations; therefore, an in-depth analysis of the number of observations recorded in individual epochs of the observation files is indispensable.

Figure 4 shows the number of GPS, GLONASS, and Galileo satellites with available observations on one and on two frequencies for the receivers BX03 and BX07. Notice that the number of available satellites sometimes drops to zero. The largest number of such breaks can be seen on days 84 and 87. Thus, to illustrate this phenomenon more precisely, we decided to additionally present day 84 as an example showing this phenomenon. The gaps are short and occur simultaneously for all types of observations of a given system. The largest number of gaps occurs for the GPS and Galileo systems, while the smallest for the GLONASS, for which gaps occur very rarely. Figure 4 shows two stations to present differences in the number of gaps occurrence. The BX07 receiver recorded observation data almost continuously with individual epochs where GPS or Galileo observations were missing. The BX03 receiver, on the other hand,

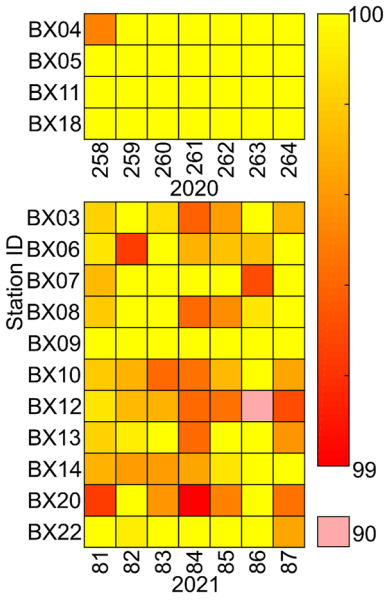

Figure 3: Observation availability for each observation epoch collected by low-cost receivers in test periods from RINEX files in % (color bar scale).

had more problems with continuous signal tracking. This receiver data are split by short interruptions in the received GNSS signal. Both receivers observe these discontinuities in the data for both frequencies simultaneously. The described interruptions in signal supply may be caused by hardware or software problems of some receivers used in the experiment. Nevertheless, all prototype receivers were configured in the same way, which may indicate technical problems only at some stations, which are difficult to identify.

Figure 5 shows the mean number of satellites observed by low-cost stations divided into three groups: (1) the number of satellites with the availability of at least one observation of any type, (2) the number of satellites for which code and phase observations on one frequency are recorded, and (3) the number of satellites for which complete observations are available on both frequencies. For comparison purposes, Figure 5 also shows the WROC EPN station, which shows the same analysis for a geodetic-grade receiver. The mean differences between the first and second groups equal 0.2 satellites. These minor differences may be related to the temporary data gaps shown in Figure 4. The most remarkable differences between the observed single-frequency and complete data are obtained for GPS. The mean difference of the GPS satellites from groups (2) and (3) exceeds 3 satellites. The low-cost GNSS receiver cannot retrieve precise P2 signals, which are the only code data at the second frequency for older GPS satellites from Block IIA and IIR. The second civilian use signal, L2C, is being broadcasted starting with the first Block IIR-M satellite launched in 2005. For Block IIA and IIR satellites, users can track only one frequency in the absence of an L2C code [33]. This fact reduces the available dual-frequency GPS constellation from 31 to 22 spacecraft and may limit the utilization of low-cost receivers with ionosphere-free linear combinations due to the lower number of observed satellites.This situation is not present for the WROC station, for which almost all available

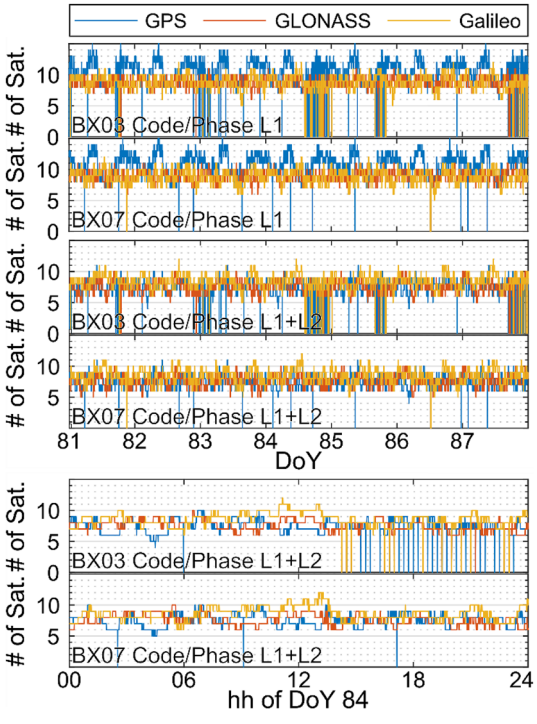

Figure 4: GPS observation availability from BX03 and BX07 low-cost receivers in DoY 81–87, 2021 (upper and middle plot). The bottom plot shows data availability in DoY 84, 2021.

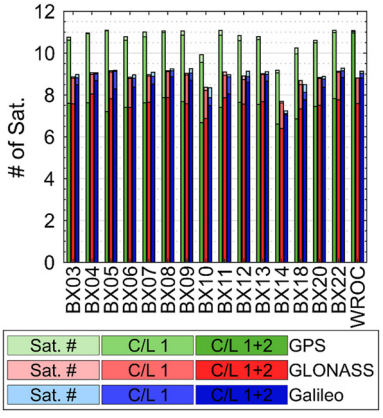

Figure 5: Mean number of satellites registered by low-cost receivers and for the WROC EPN station.

GPS satellites have always the complete set of observation data.

The mean number of GLONASS satellites in the third group is reduced by about 1.5 satellites when compared to the second group. This is because the observations at the second frequency are not recorded for satellites R06, R10, and R23. A slightly lower number of Galileo satellites with a complete set of observations was stored in RINEX files, which is mainly due to the fact that the E20 satellite (GSAT0104) transmits a single-frequency E1 signal [34]. It shows the lack of used receiver dependency, which is proved by the data presented for the WROC station for which observation for GLONASS and Galileo also contains fewer data for the second frequency. In summary, the mean number of visible satellites for which low-cost GNSS receivers record dual-frequency data is 7.4, 7.4, and 8.4 for GPS, GLONASS, and Galileo, respectively.

Additionally, the average daily number of cycle-slips is computed using single frequency cycle-slip detector and with geometree-free combination to illustrate the quality of the observations provided by the low-cost receivers. Figure 6 presents the average number of cycle-slips detected for the low-cost receivers. What is more, the average number of cycle-slips for the EPN WROC station is shown to illustrate observation quality in terms of their continuity of the geodetic grade receivers. GLONASS has the biggest number of cycle-slips among the tested receivers and reaches up to 1100 signal jumps for BX05. The average number of cycle-slips for all low-cost receivers is equal to 331, 585, and 251 for GPS, GLONASS, and Galileo, respectively. These values are significantly higher compared to the WROC station for which cycle-slips occur in 11, 35, and 12 epochs for GPS, GLONASS, and Galileo, respectively. The large amount of signal cycle-slips present in data stored by low-cost receiver is a serious problem that limits the resolution of phase ambiguity computation, especially for the GLONASS system.

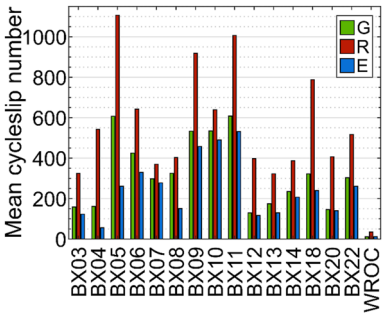

Figure 6: The daily average number of cycle-slips detected for the low-cost receiver and WROC station.

4 Evaluation of relative GNSS positioning

The data collected by the tested low-cost GNSS receivers have been tested in relative positioning. The results obtained are presented in the subsections of the chapter.

4.1 Processing strategy

The data collected during the measurement campaigns are first used to determine the baselines between the GNSS receivers. The computations are conducted in the Leica Infinity 3.3.2 (LI) software commonly used for the realization of local geodetic control networks. Different session lengths and different strategies are tested to verify the usefulness of low-cost GNSS receivers. Table 2 summarizes the session lengths, GNSS constellations, and calculated baseline types. As mentioned in Section 2 three sets of observation data stored by different types of receivers are used in the presented paper: low-cost, EPN stations, and geodetic-grade. These three sets of data allowed the following baseline types to be determined: baselines between two low-cost receivers – UBX–UBX, baselines between low-cost and EPN stations – UBX–EPN, and baselines between two geodetic-grade receivers – GEO–GEO. The last type of baseline is presented for comparison purposes to illustrate the quality difference between the use of professional and low-cost equipment. Those observation data allow us to create baselines in the range between 0 and 450 km depending on the receivers' distribution. All computed baselines are divided into three groups based on their length: short baselines for the range of 0–15 km, medium baselines in the range of 15–25 km, and long baselines longer than 25 km. For long baselines, calculations are limited to daily and hourly sessions. Table 3 shows the calculation strategy used in LI.

4.2 Characteristic of the computed baselines

The first step is to determine the percentage of integer-resolved phase ambiguities for different baselines which indicates the reliability of baseline estimation.

The number of vectors that obtained the "Phase Fixed" status varies and depends on the calculation variant. Figure 7 shows the percentage of fixed vectors for each calculation variant. The data presented are divided according to the type of baseline (UBX–UBX, UBX–EPN, and GEO–GEO) and the duration of the observing session. Each bar depicts the results obtained for a specific processing

Table 2: Characteristics of the calculation variants used in the experiment.

Processing variants		
	Session length	**Constellation**
DoY 258–264, 2020 DoY 81–87, 2021	60 min, 24 h	GPS (G), GPS + GLONASS + Galileo (GRE)
DoY 262, 2020 DoY 86, 2021	10 min, 20 min, 30 min, 60 min	
Baseline variants	UBX–UBX, UBX–EPN, UBX–WROC	

Table 3: Characteristics of the calculation strategies used in Leica Infinity software 3.3.2.

Elevation cut-off angle	10°
Orbits	CODE MGEX final products "COD0MGXFIN" [35]
Antenna calibration	Absolute antenna calibration igs14.atx for EPN stations, no calibrations for u-blox antennas
Frequencies	L1 (only for baselines in range 0–25 km); ionosphere-free (IF [36]) linear combination based on code and phase L1 and L2 (GPS, GLONASS) or E1 and E5b (Galileo) for baselines >25 km
Tropospheric model	Global pressure and temperature model 2 (GPT2, [37])

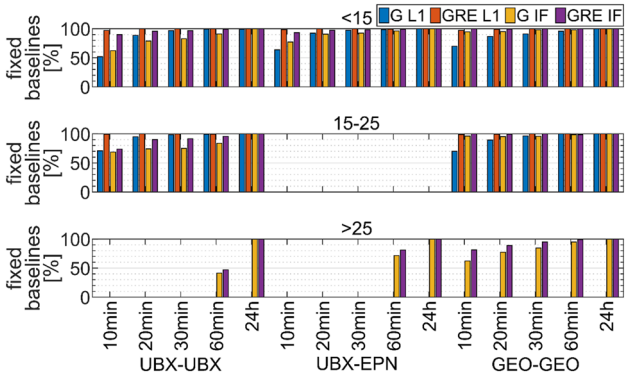

Figure 7: Percentage share of fixed short (top panel), medium (middle panel), and long (bottom panel) baselines for each calculation variant.

strategy, where G stands for GPS-only processing and GRE stands for GPS + GLONASS + Galileo, L1 represents single frequency processing, and IF indicates ionosphere-free linear combination. The top panel of Figure 7 presents results for short baselines, the middle panel presents results for medium-length baselines, and the bottom panel shows results for long baselines. The average number of fixed short baselines using the GPS in 10 min sessions is 52% and 64% for the UBX–UBX and UBX–EPN vectors, respectively. In the case of the GRE L1 solution, 10 min observations allow for determining 97% of the baselines. A similar level of effectiveness is achievable for the GPS L1 solution with at least 30 min observations. The number of fixed short and medium baselines in the G IF variant is smaller than in the case of G L1 solutions. In the case of long baselines, 60 min sessions allow for fixing only 44 and 59% of the calculated UBX-UBX vectors for variant G and GRE, respectively. An improvement is seen in the case of the UBX–EPN vectors, for which the number of vectors fixed is 72% and 81% for variant G and GRE, respectively. Note that when using GLONASS observations, ambiguities are fixed only for baselines with at least one geodetic-grade receiver. However, it is still possible to obtain a fixed status based on the GPS and Galileo systems between two low-cost receivers.

The number of baselines with fixed ambiguities decreases along with the shortening of the observation session. Additionally, more fixed baselines from the range between 0 and 25 km are computed using the L1 frequency than the ionosphere-free combination. The reduced number of fixed ambiguities for ionosphere-free linear combination is related to the lower number of observations as shown Figure 5. Moreover, the ionosphere-free wavelength (10.7 cm) is shorter than the L1 wavelength (19.4 cm) [38], and the longer wavelength is, the more precise ambiguities occur [39]. The shorter wavelength combined with the increased noise of the ionosphere-free combination reduces the number of the determined ambiguities. The results for short baselines show a very similar number of fix baselines with 1% differences for the same baselines length and session duration, regardless of whether the baseline contains an EPN station or is determined only by two low-cost receivers. The positive effect of employing EPN stations in the 60 min session is noticeable in the case of long baselines, for which 82% of the computed baselines obtained the fix status in the GRE variant. When comparing the UBX–EPN

baselines with the UBX–UBX baselines, the gain is equal to 70%. The importance of using the GRE solution increases in inverse proportion with the duration of the session length. This is visible in the case of 10-min sessions for UBX–UBX baselines, for which the gain resulting from the use of GRE observations is equal to 87%. This gain of using GRE data is clearly visible in the case of short UBX–UBX baselines, for which the number of fixed ambiguities is comparable to the result obtained by the GEO–GEO baselines.

4.3 Repeatability of the baselines length

In the next step, the repeatability of the computed baselines is verified for all variants. Standard deviation (StdDev) for the length of the unique baselines is adopted as an indicator of repeatability. StdDev is calculated from the mean differences of the unique baselines to the mean length of each unique baseline. Please note that in the case of daily sessions the number of observations is much smaller than in the case of sub-daily sessions. Figure 8 illustrates the repeatability for the analyzed baselines in relation to their length. Due to minor differences between the results obtained in short sessions and the lack of the visible session length pattern, results for sub-daily sessions are aggregated into a common group for simplification.

The results in daily sessions allow for achieving better baseline repeatability than in the case of short observation sessions. Short baselines in 24 h sessions have a StdDev smaller than 1.5 mm in most cases. When the ionosphere-free combination is used, the repeatability of the results for short and medium baselines decreases by a factor of two, and the StdDev value differences increase for baselines of similar length. The negative impact of using the ionosphere-free combination is pronounced for the short and medium baselines in sub-daily sessions. For short sessions in the L1 strategy, the results deteriorate with increasing baseline length, reaching an error of 8 mm for baselines up to 25 km. Further increasing the length of the baseline reduces the quality of the obtained results, which in most cases does not exceed 20 mm for 24 h observation sessions, while for sub-daily sessions, it allows for achieving the repeatability of 100 mm. The positive impact of using the GRE combination is more visible in short sessions than in daily sessions when computing long baselines.

Figure 9 illustrates the StdDev aggregated values of the length differences obtained for the calculated baselines in daily sessions. Among the GEO–GEO computed baselines there were 4, 3, and 4 vectors in the range below 15, 15–25, and more than 25 km, respectively. The figure demonstrates high repeatability of the results obtained for short baselines, equal 0.6 mm and 0.7 mm in L1 solutions in the UBX–EPN and UBX–UBX 2021 baselines, respectively. The repeatability of the medium baselines is slightly worse and exceeds the value of 1 mm. The results obtained for the 2020 data for short and medium baselines are based on two and one unique baselines, respectively, which can result in larger errors for these baselines. The repeatability for short baselines calculated on the ionosphere-free combination is below 1.5 mm and below 1 mm, for the UBX–UBX and UBX–EPN baselines, respectively. In the case of medium baselines, the repeatability of the baseline obtained is comparable to the results of geodetic grade receivers. However, the use of the ionosphere-free combination in the GEO–GEO

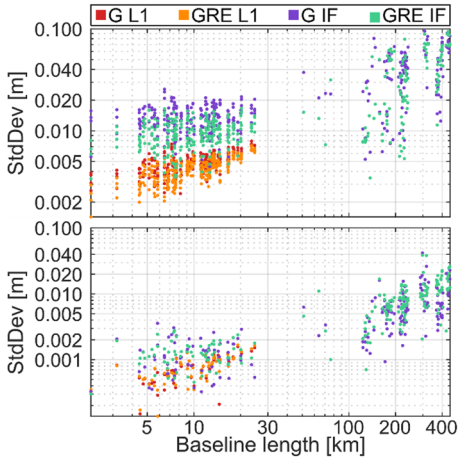

Figure 8: Repeatability of baselines for the tested strategies in subdaily (top panel) and daily sessions (bottom panel). Note the logarithmic axis scales.

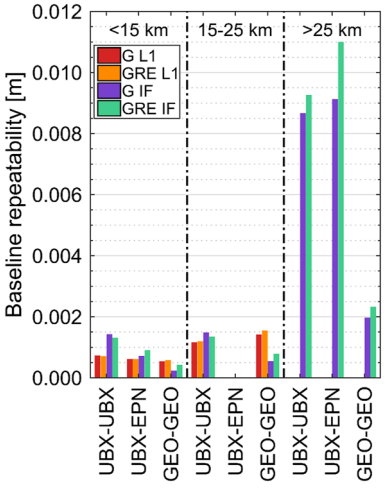

Figure 9: StdDev values of baselines length differences for daily sessions.

variant reveals the outcomes below 1 mm, which indicates the influence of the ionospheric delay seen in L1 solutions. Low-cost receivers determine 15–25 km baselines three times worse than geodetic grade receivers. The repeatability for long baselines is significantly worse and the results are comparable for G and GRE variants. The results for UBX–UBX baselines compared to the results obtained for GEO–GEO baselines are significantly less accurate and show the limitations of these devices even for baselines using EPN stations (UBX–EPN). However, short baselines created by UBX receivers reveal slightly worse results than those provided by GEO-only receivers. For short baselines, low-cost receivers provide results comparable to the results of GEO–GEO baselines. On the other hand, there is no advantage of the second frequency usage for UBX–UBX medium baselines that is observed for GEO–GEO baselines. The results of those 24 h session show the potential of the low-cost receivers in terms of densification of existing permanent networks with a limited spatial range.

Figure 10 shows the length differences for short baselines in sessions lasting from 10 to 60 min. Regardless of the duration of the observation session, short baselines are characterized by better repeatability when using one frequency, resulting in more than two times better outcomes when compared with the strategy employing the ionosphere-free combination. There is a slight repeatability gain of 6–15% and 15–23% when using GRE on a single frequency for UBX–UBX and UBX–EPN baselines, respectively. Short UBX–UBX baselines need 60 min of data to achieve repeatability comparable to the UBX–EPN baselines in 10 min sessions. For short UBX–EPN baselines in the GRE scenario give results only 1 mm worse than GEO–GEO baselines. The UBX–UBX baselines perform not as well and have 1.5 times worse results than the GEO–GEO baselines.

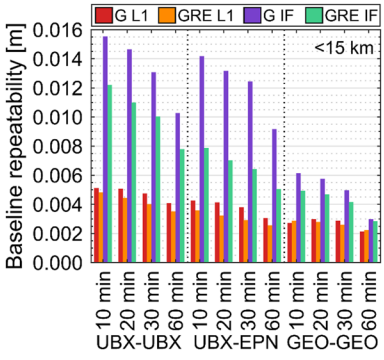

Figure 10: StdDev values of short baselines length differences for sub-daily sessions on March 27, 2021 (DoY 86, 2021).

Figure 10 shows the StdDev for short baselines length differences in sessions lasting from 10 to 60 min. The results for the 60 min sessions are equal to 3.5, 2.5, and 2.2 mm for UBX–UBX, UBX–EPN, and GEO–GEO baselines, respectively. The degradation of outcomes caused by shortening the duration of the session looks similar for the baselines UBX–UBX and UBX–EPN. In all cases in the GRE L1 variant, the use of sessions of 30 min, 20 min, and 10 min degrades the results by 15%, 10%, and 10%, respectively, with respect to the duration of the sessions of 60 min, 30 min, and 20 min, respectively. In the case of the results for GEO–GEO baselines, they deteriorate slightly less, especially in 10 and 20 min sessions. Regardless of the duration of the observation session, short baselines are characterized by better repeatability when using one frequency, resulting in more than twice better results compared to the strategy employing the ionosphere-free combination.

Figure 11 shows the StdDev for the baselines repeatability results obtained for medium (left panel) and long baselines (right panel). The time-dependent degradation for UBX–UBX in the case of medium baselines is smaller than for short baselines. The results for UBX–UBX baselines only slightly differ in various session lengths both in G and GRE scenarios. In terms of GRE variant the results improve by 5–15% with respect to GPS-only scenario. Medium GEO–GEO baselines obtained slightly bigger StdDev than UBX–UBX medium baselines due to the three unique GEO–GEO among which all baselines were longer than 20 km. In the case of ionosphere-free solutions, there is a positive effect associated with the use of multi-GNSS observations. For long baselines created with low-cost receivers the results can be improved by applying PCO and PCV corrections with a few millimeters [28]. Nevertheless,

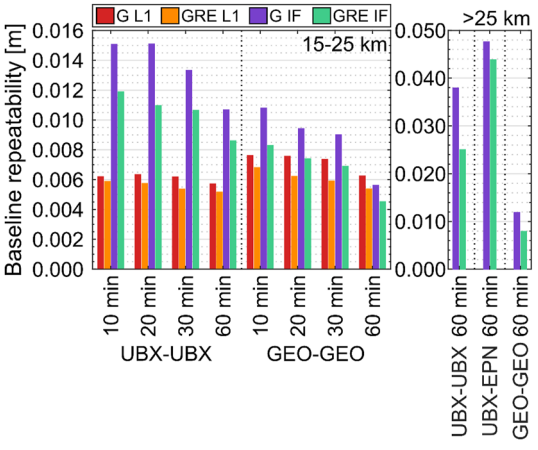

Figure 11: StdDev values of medium and long baselines length differences for sub-daily sessions on March 27, 2021 (DoY 86, 2021).

the multi-GNSS solution provides more accurate results than the GPS-only solution in both baseline types based on low-cost receivers and geodetic class receivers. It should be noted that the number of unique UBX–EPN was 121, while the amount of baselines for UBX–UBX baselines was only 12. The worse results may be additionally influenced by the longer lengths of the UBX–EPN baselines. Shorter sessions allow for creating short baselines with a good length repeatability. However, it is worth using a multi-GNSS solution and one geodetic receiver to increase the repeatability of the results. On the other hand, in terms of long baseline creation low-cost receivers should not be used even when two frequencies multi-GNSS scenario is applied. It is visible that the results for long baselines created with at least one UBX receiver perform three to five times worse than the GEO–GEO baselines. Therefore, the use of this equipment for baselines longer than 25 km is not recommended.

4.4 Relative positioning coordinates

The coordinates of the low-cost receivers were also determined in the network solution in relation to the WROC station. Two 12 h sessions for every day from period DoY 81–87, 2021 were used. The second determination of the coordinates used two 1 h sessions for each day in the same period. The solution for both variants was based on the same baseline system. Figure 12 shows the obtained results of the coordinates. It can be noticed that the daily results (top panel) are in the sub-millimeter level for the horizontal components. In the case of the height component, the results are worse, but mostly they remain within the 2 mm range. The only exception is the BX20 station, for which the height component is in the range of ±8 mm.

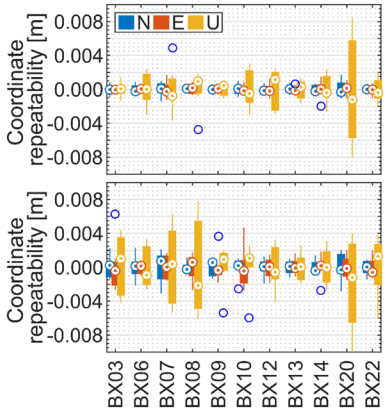

Figure 12: Coordinate repeatability for the low-cost receivers in DoY 81–87, 2021. The upper panel shows the results obtained using two 12 h sessions, the lower panel presents the results obtained with two 1 h sessions for each day of the test period.

Two 1 h sessions (bottom panel) provided poorer repeatability of the obtained coordinates with respect to the result based on daily data. In the case of two 1 h sessions (bottom panel), horizontal components obtained values are in the range of 1–2 mm. The errors in the height component also increased compared to long sessions and are in the range of 2–10 mm.

5 Absolute accuracy

The analysis presented in the previous sections shows that low-cost GNSS receivers may have great application potential in the realization of surveyor tasks. Therefore, another field experiment is conducted with the purpose of revealing possible accuracies in the realization of a geodetic control network with the use of low-cost GNSS receivers.

First, the network measurements are based on a set of seven geodetic-grade receivers. The results of this stage are used as a reference for the second variant of the test. In the test variant, the same points are measured once again in static mode; however, three geodetic receivers are replaced with low-cost receivers. The planned network consists of seven marked points near the WROC EPN station. The maximum distance of the new points from the WROC station does not exceed 400 m. Table 4 presents the characteristics of the measurement campaigns, whereas Figure 13 illustrates the distribution of network points and the generated baselines.

The calculations are conducted in the LI software. Short vectors are computed using a single frequency, whereas long vectors are computed using the ionosphere-free linear combination. The stations of the Polish GNSS permanent network, ASG-EUPOS, are used for a realization of a local reference frame: KEPN, KROT, LEGN, OPLE, WROC. Reference baselines are generated using geodetic-grade receivers due to the increased error of long vectors containing low-cost receivers, as discovered in the previous sections. Contrary to previous tests in which most low-cost antennas were located

Table 4: Description of the GNSS test campaigns.

Reference	
Session length	2 × 1 h
Interval	1 s
Receivers/antennas	7 geodetic-grade
Experimental	
Session length	2 × 1 h
Interval	1 s
Receivers/antennas	4 geodetic-grade + 3 low-cost

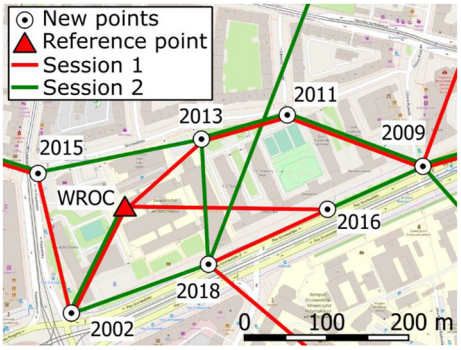

Figure 13: Distribution of network points and computed baselines.

Figure 14: The method of mounting the u-blox patch antenna on the tribrach.

on the roofs of buildings, in this experiment, the antennas were located on surveying tripods; thus, the GNSS signal could also be affected by the urban environment and the tall surrounding buildings. We apply a flat circular ground plane provided with the antenna by the manufacturer with diameter equals 10 cm. Figure 14 illustrates the method of mounting the u-blox patch antenna on the tribrach, whereas Table 5 summarizes the calculation strategies in LI.

For the horizontal network constraining, we employ five GNSS reference stations from the ASG-EUPOS network, whereas the heights are constrained by the results of precise leveling at points 2013 and 2018 of the established network with a connection to the national height geodetic network. For geoid undulations, we employ the geoid model consistent with the realization of the European Vertical Reference Frame EVRF2007-NH for the area of Poland. The calculations started with checking the quality of the baselines computed in a network and ended with a constrained adjustment of the network. Table 6 shows the coordinate differences between the test and reference campaigns. Height results are missing for the points 2013 and 2018 because these are used as height reference points.

The best results are obtained for the north coordinate component with the maximum deviation of 17 mm for the point 2013. The differences for the east component do not exceed 5 mm for points occupied by the low-cost receivers; however, some horizontal inconsistency might affect two points occupied by the geodetic-grade receivers, 2009 and 2015, with differences equal 55 mm. For the up component, all offsets are negative compared to the reference campaign; however, low-cost receivers allow for obtaining results with a maximum difference of 40 mm. The results of the experiment show that low-cost receivers can provide coordinates with a maximum difference of 17 and 41 mm for 2D and 3D positions, respectively. The presented results may be affected by the application of inadequate antenna shielding. In the literature, the experiments dedicated to this issue suggest the use of larger ground planes or even choke ring constructions commonly used on GNSS permanent stations. The choke ring may reduce the position standard deviation by about 30–40% with reference to the ground-plane shielding approach [40]. Furthermore, the multipath reduction algorithms dealing with the reflections from the obstacles located above the antenna [41] could improve the accuracy. Nevertheless, this approach is limited because it needs implementation in the processing software. Additionally, the presented results may be affected by the lack of low-cost antenna calibration files. In this paper, we decided to disregard the available calibration [28] due to its inconsistency with the official data distributed by the manufacturer.

Table 5: Characteristics of the calculation strategies used in the Leica Infinity software 3.3.2.

Systems	GPS, GLONASS, Galileo
Elevation angle	10°
Orbits	CODE MGEX final products "COD0MGXFIN" [35]
Antenna calibration	Absolute NGS antenna calibration for EPN stations and geodetic grade antennas, no calibrations for u-blox antennas
Strategy	L1 (only for short baselines) and ionosphere-free linear combination for baselines >25km
Tropospheric model	GPT2

Table 6: Position differences obtained for network points with respect to the results obtained in the reference campaign. The results for low-cost receivers are highlighted in bold.

	dN [m]	dE [m]	dU [m]
2002	**0.005**	**0.005**	**−0.040**
2009	0.009	0.055	−0.006
2011	0.005	−0.012	−0.009
2013	**0.017**	**−0.002**	**–**
2015	−0.005	0.055	−0.021
2016	**0.016**	**−0.001**	**−0.031**
2018	0.010	0.000	–

6 Conclusions

The results presented in this paper demonstrate the utility potential of low-cost u-blox C099-F9P receivers equipped with the ANN-MB series patch antenna. Analysis of the content of RINEX files generated by the low-cost receivers discloses some limitations resulting from the lack of tracking of the entire GPS constellation because of the absence of the civil code L2C on the second frequency for the older class GPS satellites. The results show the highest reliability and repeatability for daily sessions. However, from a practical point of view, the use of such long sessions may be unjustified in everyday works related, for example, to the establishment of geodetic control networks. The greatest benefit of using the multi-GNSS constellations compared to GPS-only is visible in 10 min observation sessions. For multi-GNSS computation variants the number of fixed baselines increases by 40% in 10 min session when compared to GPS-only variant. The presented results confirm the high potential of low-cost receivers for the densification of geodetic control networks in an area of up to 25 km and demonstrate the limitation of reliability for long baselines. The length differences for the baselines longer than 25 km is at the centimeter level accuracy, which corresponds to the results obtained for a single long baseline [31]. Furthermore, the use of one geodetic-grade receiver in a short baseline improves repeatability by 20% compared to a baseline measured with two low-cost receivers. The second frequency makes it possible to create an ionosphere-free combination; however, the results presented in the paper show that the quality of long baselines is much lower compared to baselines determined with the use of geodetic grade receivers. This fact proves the lesser potential of the low-cost receivers in long baseline creation. The field experiment conducted to establish the local geodetic control network with a mixture of geodetic-grade and low-cost receivers shows that the coordinate accuracy is better than 17 mm and 40 mm for horizontal and vertical component, respectively.

Although some papers report better accuracies [40, 42], it is mainly because of the extended session lengths and the use of geodetic-grade receivers as a base station.

The number of baselines with fixed phase ambiguities and the high repeatability of the determined baseline lengths confirm the usefulness of observations recorded with low-cost receivers, especially for the determination of short baselines. However, geodetic measurements require robustness and integrity, which are still an issue in the case of low-cost receivers. This issue may be solved by the application of better quality antennas, advanced shielding or algorithms reducing multipath effect.

The potential of low-cost GNSS receivers prompts reflection on the possible applications in surveying and geodetic work when setting up control and reference networks. Their usefulness can be even greater in the context of practical applications that require less accurate results at the centimeter level, such as precision agriculture, the steering of construction machines, or transport machines in the areas of container reloading.

Author contributions: All the authors have accepted responsibility for the entire content of this submitted manuscript and approved submission.

Research funding: This work has been supported by the National Science Center, Poland (UMO-2019/35/B/ST10/00515). The authors acknowledge the U + GEO company (uplusgeo.pl) for providing low-cost GNSS receivers. The geodetic grade receiver data was collected by the infrastructure of the EPOS-PL, European Plate

Observing System POIR.04.02.00–14-A003/16, funded by the Operational Programme Smart Growth 2014–2020, Priority IV: Increasing the research potential, Action 4.2: Development of modern research infrastructure in the science sector, and co-financed by European Regional Development Fund. The observation data from this study are available from the corresponding author for academic purposes upon reasonable request. The final CODE products were used in the research.

Conflict of interest statement: The authors declare no conflicts of interest regarding this article.

References

1. Altamimi Z, Métivier L, Rebischung P, Rouby H, Collilieux X. ITRF2014 plate motion model. Geophys J Int 2017;209:1906—12.
2. Geremia-Nievinski F, Hobiger T, Haas R, Liu W, Strandberg J, Tabibi S, et al. SNR-based GNSS reflectometry for coastal sea-level altimetry: results from the first IAG inter-comparison campaign. J Geodes 2020;94:1—15.
3. Hadas T, Hobiger T, Hordyniec P. Considering different recent advancements in GNSS on real-time zenith troposphere estimates. GPS Solut 2020;24424:1—14.
4. Rovira-Garcia A, Juan JM, Sanz J, González-Casado G, Ibáñez D. Accuracy of ionospheric models used in GNSS and SBAS: methodology and analysis. J Geodes 2016;90:229—40.
5. Shen N, Chen L, Wang L, Hu H, Lu X, Qian C, et al. Short-term landslide displacement detection based on GNSS real-time kinematic positioning. IEEE Trans Instrum Meas 2021;70:1—14.
6. Šegina E, Peternel T, Urbancic T, Realini E, Zupan M, Jez J, et al. Monitoring surface displacement of a deep-seated landslide by a low-cost and near real-time GNSS system. Rem Sens 2020;12:1—26.
7. Knight PJ, Bird CO, Sinclair A, Plater AJ. A low-cost GNSS buoy platform for measuring coastal sea levels. Ocean Eng 2020;203:107198.
8. GSA. GNSS market report - issue 6; 2019.
9. Gadhave SN, Kale SD, Shinde SN, Amol P, Bhosale C. Electronic jacket for women safety. Int Res J Eng Technol 2017;04:858—61.
10. Szot T, Specht C, Dabrowski PS, Specht M. Comparative analysis of positioning accuracy of Garmin Forerunner wearable GNSS receivers in dynamic testing. Measurement 2021;183:109846.
11. Banville S, van Diggelen F. Precise positioning using raw GPS measurements from android smartphones. GPS World; 2016: 43—8 pp.
12. Paziewski J. Recent advances and perspectives for positioning and applications with smartphone GNSS observations. Meas Sci Technol 2020;31:091001.
13. Paziewski J, Sieradzki R, Baryla R. Signal characterization and assessment of code GNSS positioning with low-power consumption smartphones. GPS Solut 2019;23:98.
14. Zumberge JF, Heflin MB, Jefferson DC, Watkins MM, Webb FH. Precise point positioning for the efficient and robust analysis of GPS data from large networks. J Geophys Res Solid Earth 1997;102:5005—17.
15. Gill M, Bisnath S, Aggrey J, Seepersad G. Precise Point Positioning (PPP) using low-cost and ultra-low-cost GNSS receivers. In: 30th International technical meeting of the satellite division of the Institute of navigation, ION GNSS 2017; 2017, vol 1:226—36 pp.
16. Robustelli U, Paziewski J, Pugliano G. Observation quality assessment and performance of GNSS standalone positioning with code pseudoranges of dual-frequency android smartphones. Sensors 2021;21:2125.
17. Garrido-Carretero MS, de Lacy-Pérez de los Cobos MC, Borque-Arancón MJ, Ruiz-Armenteros AM, Moreno-Guerrero R, Gil-Cruz AJ. Low-cost GNSS receiver in RTK positioning under the standard ISO-17123-8: a feasible option in geomatics. Meas J Int Meas Confed 2019;137:168—78.
18. Tsakiri M, Sioulis A, Piniotis G. The use of low-cost, single-frequency GNSS receivers in mapping surveys. Surv Rev 2016;50:46—56.
19. Odolinski R, Teunissen PJG. Low-cost, high-precision, single-frequency GPS—BDS RTK positioning. GPS Solut 2017;21:1315—30.
20. Günther J, Heunecke O, Pink S, Schuhbäck S. Developments towards a low-cost Gnss based sensor network for the monitoring of landslides. In: Proceedings of the 13th FIG International symposium on deformation measurements and analysis, Lisbon, Portugal; 2008:12—5 pp.
21. Zhao C, Yuan Y, Zhang B, Li M. Ionosphere sensing with a low-cost, single-frequency, multi-GNSS receiver. IEEE Trans Geosci Rem Sens 2019;57:881—92.
22. Singh Gill M. GNSS precise point positioning using low-cost GNSS receivers, [MSc. thesis]. Toronto: York University; 2018.
23. Biagi L, Grec FC, Negretti M. Low-cost GNSS receivers for local monitoring: experimental simulation, and analysis of displacements. Sensors 2016;16:2140.
24. Odolinski R, Teunissen PJG. Low-cost, 4-system, precise GNSS positioning: a GPS, Galileo, BDS and QZSS ionosphere-weighted RTK analysis. Meas Sci Technol 2017;28:125801.
25. Takasu T, Yasuda A. Evaluation of RTK-GPS performance with low-cost single-frequency GPS receivers. In: Proc. int. symp. GPS/GNSS; 2008:852—61 pp. [Online]. Available from: http://www.gnss-pnt.org/symposium2008/abstract/oral/B12a/7-727-a.pdf [Accessed 10 Sep 2021].
26. Poluzzi L, Tavasci L, Corsini F, Barbarella M, Gandolfi S. Low-cost GNSS sensors for monitoring applications. Appl Geomatics 2019;12:35—44.
27. Caldera S, Realini E, Barzaghi R, Reguzzoni M, Sansò F. Experimental study on low-cost satellite-based geodetic monitoring over short baselines. J Survey Eng 2016;142:04015016.
28. Krietemeyer A, van der Marel H, van de Giesen N, ten Veldhuis M-C. High quality zenith tropospheric delay estimation using a low-cost dual-frequency receiver and relative antenna calibration. Rem Sens 2020;12:1393.
29. Odolinski R, Teunissen PJG. Best integer equivariant estimation: performance analysis using real data collected by low-cost, single- and dual-frequency, multi-GNSS receivers for short- to long-baseline RTK positioning. J Geodes 2020;94:1—17.
30. Wielgocka N, Hadas T, Kaczmarek A, Marut G. Feasibility of using low-cost dual-frequency GNSS receivers for land surveying. Sensors 2021;21:1956.
31. Catania P, Comparetti A, Febo P, Morello G, Orlando S, Roma E, et al. Positioning accuracy comparison of GNSS receivers used for

mapping and guidance of agricultural machines. Agronomy 2020;10:924.
32. Vana S, Bisnath S. Enhancing navigation in difficult environments with low-cost, dual-frequency GNSS PPP and MEMS IMU. In: International association of geodesy symposia. Berlin/Heidelberg, Germany: Springer; 2020.
33. Nie Z, Liu F, Gao Y. Real-time precise point positioning with a low-cost dual-frequency GNSS device. GPS Solut 2020;24:9.
34. Steigenberger P, Montenbruck O. Galileo status: orbits, clocks, and positioning. GPS Solut 2017;21:319—31.
35. Prange L, Orliac E, Dach R, Arnold D, Beutler G, Schaer S, et al. CODE's five-system orbit and clock solution—the challenges of multi-GNSS data analysis. J Geodesy 2017;91:345—60.
36. Odijk D. Ionosphere-free phase combinations for modernized GPS. J Survey Eng 2003;129:165—73.
37. Lagler K, Schindelegger M, Böhm J, Krásná H, Nilsson T. GPT2: empirical slant delay model for radio space geodetic techniques. Geophys Res Lett 2013;40:1069—73.
38. Schaer S. Mapping and predicting the Earth's ionosphere using the Global Positioning. Zürich: Schweizerische Geodätische Kommission; 1999, vol 59.
39. Odijk D, Teunissen PJG, Tiberius CCJM. Triple-frequency ionosphere-free phase combinations for ambiguity resolution; 2002. [Online]. Available from: https://www.researchgate.net/publication/265675825 [Accessed 17 Feb 2022].
40. Zhang L, Schwieger V. Investigation of a L1-optimized choke ring ground plane for a low-cost GPS receiver-system. J Appl Geodesy 2018;12:55—64.
41. Chen J, Li H, Wu B, Zhang Y, Wang J, Hu C. Performance of real-time precise point positioning. Mar Geodesy 2013;36:98—108.
42. Romero-Andrade R, Trejo-Soto ME, Vega-Ayala A, Vázquez-Ontiveros JR, Sharma G. Positioning Evaluation of Single and Dual-Frequency Low-Cost GNSS Receivers Signals Using PPP and Static Relative Methods in Urban Areas. Appl Sci 2021;11. https://doi.org/10.3390/app112210642.